

# Dynamics of beryllium-7 specific activity in relation to meteorological variables, tropopause height, teleconnection indices and sunspot number

D. Sarvan<sup>a,\*</sup>, Đ. Stratimirović<sup>b,c</sup>, S. Blesić<sup>d,c</sup>, V. Djurdjevic<sup>e</sup>, V. Miljković<sup>f</sup>,  
J. Ajtić<sup>a,c,\*\*</sup>

<sup>a</sup>*University of Belgrade, Faculty of Veterinary Medicine, Bulevar oslobođenja 18, 11 000 Belgrade, Serbia*

<sup>b</sup>*University of Belgrade, Faculty of Dental Medicine, Dr Subotića 8, 11 000 Belgrade, Serbia*

<sup>c</sup>*Institute for Research and Advancement in Complex Systems, Zmaja od Noćaja 8, 11 000 Belgrade, Serbia*

<sup>d</sup>*Department of Environmental Sciences, Informatics and Statistics, Ca'Foscari University of Venice, Mestre, Italy*

<sup>e</sup>*University of Belgrade, Faculty of Physics, Institute of Meteorology, Studentski trg 12, 11 000 Belgrade, Serbia*

<sup>f</sup>*University of Belgrade, Faculty of Physics, Studentski trg 12, 11 000 Belgrade, Serbia*

---

## Abstract

The dynamics of the beryllium-7 specific activity in surface air over 1987–2011 is analyzed using wavelet transform (WT) analysis and time-dependent detrended moving average (tdDMA) method. WT analysis gives four periodicities in the beryllium-7 specific activity: one month, three months, one year, and three years. These intervals are further used in tdDMA to calculate local autocorrelation exponents for precipitation, tropopause height and teleconnection indices. Our results show that these parameters share common periods with the beryllium-7 surface concentration. tdDMA method indicates that on the characteristic intervals of one year and shorter, the beryllium-7 specific activity is strongly autocorrelated. On the three-year interval, the beryllium-7 specific activity shows periods of anticorrelation, implying slow changes in its dynamics

---

\*Corresponding author

\*\*Principal corresponding author

*Email addresses:* [darko.sarvan@vet.bg.ac.rs](mailto:darko.sarvan@vet.bg.ac.rs) (D. Sarvan),  
[dj.stratimirovic@gmail.com](mailto:dj.stratimirovic@gmail.com) (Đ. Stratimirović), [suzana.blesic@unive.it](mailto:suzana.blesic@unive.it) (S. Blesić),  
[vdj@ff.bg.ac.rs](mailto:vdj@ff.bg.ac.rs) (V. Djurdjevic), [vladimir.miljkovic@ff.bg.ac.rs](mailto:vladimir.miljkovic@ff.bg.ac.rs) (V. Miljković),  
[jelena.ajtic@vet.bg.ac.rs](mailto:jelena.ajtic@vet.bg.ac.rs) (J. Ajtić)

that become evident only over a prolonged period of time. A comparison of the Hurst exponents of all the variables on the one- and three-year intervals suggest some similarities in their dynamics. Overall, a good agreement in the behavior of the teleconnection indices and specific activity of beryllium-7 in surface air is noted.

*Keywords:* beryllium-7, wavelet analysis, periodicities, Hurst exponent, long-range correlations

---

## 1. Introduction

Beryllium-7 (half-life 53.22 days) is a naturally occurring radionuclide that is produced in the upper troposphere (around 30 %) and lower stratosphere (around 70 %) [1]. After formation  $^7\text{Be}$  attaches to fine aerosols, and its residence time in the atmosphere is long [2, 3, 4, 5]. The ensuing transport of the aerosols, and therefore of the radionuclide, is governed by the atmospheric circulation [6, 7].

Concentration of  $^7\text{Be}$  in any given location (altitude, latitude, longitude) depends on several factors [8]. First, the source of the radionuclide is its production in the higher layers of the atmosphere. Therefore, the production rate influences the total amount of the radionuclide. Second, transport can increase or decrease the radionuclide concentration at a particular location, depending on abundance of  $^7\text{Be}$  in the transported air masses. Finally, the rate of the isotope removal influences its concentration in the atmosphere.

The above mechanisms have been investigated. Monthly  $^7\text{Be}$  specific activities in surface air are inversely correlated with solar activity [6, 9, 10]. Air masses originating in the upper troposphere and lower stratosphere contain higher concentrations of  $^7\text{Be}$  than surface air masses [11]. Beryllium-7 can thus be used as a stratospheric tracer, and has been investigated as an indicator of exchange processes between the stratosphere and troposphere [12, 7]. Further, the  $^7\text{Be}$  concentration maxima have been correlated with an enhanced vertical transport and the intrusion of the stratospheric air masses across the tropopause

[13, 14, 15, 16]. A positive correlation between the tropopause height and the  $^7\text{Be}$  specific activity in surface air has been shown [17, 18]. Longitudinal and latitudinal distribution of  $^7\text{Be}$  in the air has been noted [8, 19, 20, 21], and it is in part influenced by horizontal transport within the troposphere. Wet deposition is the most significant mechanism of  $^7\text{Be}$  removal from the atmosphere [10, 22, 23], although different studies have shown no correlation or a negative correlation of the  $^7\text{Be}$  specific activity with precipitation [6, 10, 24, 25, 26, 27].

To further explain the behavior of  $^7\text{Be}$  in surface air, its relation to local climate variables, including (but not limited to) temperature, atmospheric pressure, relative humidity, and sunshine hours, has been extensively studied [22, 13, 28, 29, 30, 10, 31, 32, 33, 34]. These studies, however, did not include an analysis of  $^7\text{Be}$  relation with large-scale atmospheric circulation.

Variability in atmospheric circulation is described by teleconnection patterns, such as the North Atlantic Oscillation (NAO), Arctic Oscillation (AO) and Pacific/North American (PNA) [35, 36]. These patterns are a measure of pressure oscillations over different locations, and have been shown to influence large-scale circulation [37, 38, 39], which further reflects on local weather conditions [40, 41, 42, 43].

An influence of NAO on  $^7\text{Be}$  has been implied [7, 44], but only relatively recent studies have focused on the  $^7\text{Be}$  specific activity in the air and large-scale transport. For example, the abundance of  $^7\text{Be}$  in Fennoscandia is not only influenced by NAO [45, 46], but the atmospheric conditions seem to play a more important role than production [47]. Further, AO can modulate the stratosphere-troposphere exchange, and as a consequence, the AO variability can explain a large part of ozone variability in the lower troposphere over North America [48]. This finding is also relevant for  $^7\text{Be}$  which is, along with ozone, transported from the stratosphere into troposphere.

To summarize, there have been a number of studies on the  $^7\text{Be}$  specific activity in surface air and its relation with local meteorological conditions, sunspot number, and tropopause height, and somewhat fewer studies on the influence of large-scale atmospheric transport. Most of these studies looked into linear

relationship between the  $^7\text{Be}$  specific activity and a set of chosen variables. However, there have been no in-depth statistical analysis encompassing meteorological variables, tropopause height, sunspot number and teleconnection indices (which quantify large-scale transport). The goal of our investigation is to look into common periodicities of the mentioned variables, whose existence could help to understand a relationship between the variables, even if it may not be linear in its nature. Two statistical analysis methods are used to investigate the dynamics of the  $^7\text{Be}$  surface concentration: wavelet transform analysis and time-dependant Hurst exponent method.

## 2. Data

Time series of 11 measured variables were analyzed. The  $^7\text{Be}$  specific activity in surface air, five meteorological variables, and the tropopause height were of local character – the data were recorded in Helsinki, Finland (60.21 °N; 25.06 °E; 12 m a.s.l). On the other hand, three teleconnection indices and sunspot number quantify hemispheric circulation, and sun activity, respectively. This set of variables was chosen in attempt to include as many as possible factors potentially influencing the  $^7\text{Be}$  specific activity in surface air, but this choice was limited by the number of meteorological variables available for Helsinki, and by the temporal resolution of the available teleconnection indices. The length of the investigated time series differed, and the start and end date of the analysis were chosen to coincide with the available  $^7\text{Be}$  specific activity data – from 1 January 1987 to 31 December 2011, thus spanning 25 years.

*Beryllium-7 specific activity in surface air.* The analyzed data are a subset of the Radioactivity Environmental Monitoring Database (REMdb) supported by REM group from the Institute of Transuranium Elements, of the DG Joint Research Centre (JRC). The  $^7\text{Be}$  data prior to 2007 stored in the REMdb is public, and an access to the data over the 2007–2011 period can be granted only after explicit request. More information on the REMdb can be found on its web page (<https://rem.jrc.ec.europa.eu/>) and in [21, 49, 50]. The measurements

conducted in Helsinki represent the largest set with more than 4 000 data points over 1987–2011. The sampling frequency of the measurements varied: prior to 1999, the measurements were taken mostly once a week, while the subsequent measurements were performed daily or once in two days.

*Meteorological variables.* The meteorological data, consisting of mean, minimum and maximum temperature, atmospheric pressure, and precipitation, were obtained from the European Climate Assessment & Dataset (ECA&D) [51]. The series consisted of daily data.

*Tropopause height.* Tropopause height was calculated following the procedure given in [18]. Input data for the calculations were taken from the NCEP/NCAR reanalysis [52]. In the procedure, an extrapolation of isobaric heights above and below the tropopause to the tropopause pressure was performed using the hydrostatic approximation. The averaged value of the two extrapolated values was then taken as the height of the tropopause. The calculations of the tropopause height were performed for each day of the investigated period.

*Teleconnection indices.* The daily values of three teleconnection indices of large-scale atmospheric circulation: North Atlantic Oscillation, Arctic Oscillation, and Pacific/North American were obtained from the data archive of the United States National Oceanic and Atmospheric Administration’s Climate Prediction Center (<http://www.cpc.ncep.noaa.gov> visited on 16 April 2015).

*Sunspot number.* The daily sunspot data were obtained from the SIDC-team (World Data Center for the Sunspot Index, Royal Observatory of Belgium, Monthly Report on the International Sunspot Number, online catalogue of the sunspot index: <http://www.sidc.be/sunspot-data/1987-2011>).

### **3. Calculations**

Two statistical methods were applied in the analysis of the  $^7\text{Be}$  specific activity dynamics: wavelet transform analysis and time-dependant Hurst exponent method.

### 3.1. Wavelet analysis

Wavelet transform (WT) spectral analysis of the  ${}^7\text{Be}$  time series was used to look into existence of periodic or quasi-periodic cycles in the data [53, 54] and to assess the overall statistical behavior of the  ${}^7\text{Be}$  series [55]. The existence of cycles was then compared across the chosen datasets to find their common periodicities.

Wavelet transform analysis is commonly used as a tool to investigate time series that contain nonstationarities on a number of different frequencies [56]. The WT procedure that we used is described in [55, 57]. In this paper, a set of Derivatives of Gaussian (DOG) wavelets of the tenth order was used to calculate WT coefficients. The calculated wavelet spectra represent variations of the analyzed signals on different time scales, and show increased values for the events occurring at a characteristic time scale. To detect those characteristic scales, a standard peak analysis was performed by searching the maximum and saddle (for hidden peaks) points in the WT power spectra of the investigated variables.

### 3.2. Time-dependant Hurst exponent

Centered detrended moving average (cDMA) technique operates through an estimate of a generalized variance of the long-range correlated series  $y(i)$  around the moving average  $\tilde{y}_n(i)$ :

$$\tilde{y}_n(i) = \frac{1}{n} \sum_{k=-\frac{n}{2}}^{k=\frac{n}{2}-1} y(i-k), \quad (1)$$

where  $n$  is the width of the moving average window. The time series  $y(i)$  is detrended by subtracting the local trend  $\tilde{y}_n(i)$ , and for a given window width  $n$ , the characteristic size of fluctuation for detrended time series is calculated by:

$$\sigma_{cDMA}(n) = \sqrt{\frac{1}{N_{max} - n} \sum_{i=\frac{n}{2}}^{N_{max}-\frac{n}{2}} [y(i) - \tilde{y}_n(i)]^2}. \quad (2)$$

Function  $\sigma_{cDMA}(n)$  is calculated for different moving window widths,  $n \in [\frac{n}{2}, N_{max} - \frac{n}{2}]$ , where  $N_{max}$  is the length of the entire series. An increase in the window width  $n$  increases the function  $\sigma_{cDMA}(n)$ .

When the analyzed time series follows a scaling law, the cDMA function is of a power-law type, i.e.  $\sigma_{cDMA}(n) \propto n^H$ , where  $H$  is Hurst exponent which is related to the correlation properties of  $y(i)$ . When  $0.5 < H < 1$ , the series  $y(i)$  has a positive long-range correlation, or persistence; when  $0 < H < 0.5$ , the series has a long-range negative correlation, or anti-persistence; and when  $H = 0.5$ , the series can be described as an uncorrelated Brownian process.

Local complexity in our data sets was investigated using the time-dependent DMA (tdDMA) algorithm [58] in the following manner. First, cDMA algorithm was applied on the subset of data at the intersection of the time series signal and a sliding window with a width  $N_s$ , which moved along the series with a step  $\delta_s$ . The scaling exponent  $H$  was then calculated for each subset, following the cDMA procedure described above, and a sequence of local, time-dependent Hurst exponents was obtained. The minimum size of each subset  $N_{min}$  was defined under a condition that the scaling law  $\sigma_{cDMA}(n) \propto n^H$  holds in the subset, while the accuracy of the technique was achieved with an appropriate choice of  $N_{min}$  and  $\delta_{min}$  [59].

In our tdDMA analysis, window widths of up to  $N_s = 3265$  were chosen, with the step  $\delta_s = 1$ . The scaling features of the chosen variables were studied on four characteristic periods: one month, three months, one year, and three years. These periods enclosed the  ${}^7\text{Be}$  specific activity spectral peaks obtained by the WT analysis.

#### 4. Results and Discussion

The wavelet spectra for the  ${}^7\text{Be}$  data series were calculated in the range of 15–1500 points, corresponding to the time span of ten days to four years. This range was chosen having in mind the length of the time series analyzed (daily records in 25 years), so that we can obtain statistically relevant results [60].

Augmented Dickey-Fuller unit-root test was performed on the  $^7\text{Be}$  data series. The test showed stationarity of the data series.

#### 4.1. Characteristic periods

Four characteristic periods (corresponding to the time coordinates of the local maxima) were detected in the  $^7\text{Be}$  spectrum (Fig. 1): the peak around 30 days indicating a monthly cycle; the peak around 90 days indicating a seasonal cycle; the peak around 360 days indicating an annual cycle; and the peak around 1000 days implying a longer cycle of around three years (triennial cycle). A seasonal periodicity has already been observed in the behavior of  $^7\text{Be}$  [61, 46]. A periodicity of 45–90 days in the  $^7\text{Be}$  wavelet spectrum has also been reported before [47], as an intermittent period connected to changes in teleconnection indices. Similarly, a periodicity of  $\sim 2.5$  years in the  $^7\text{Be}$  surface concentrations has already been noted [6].

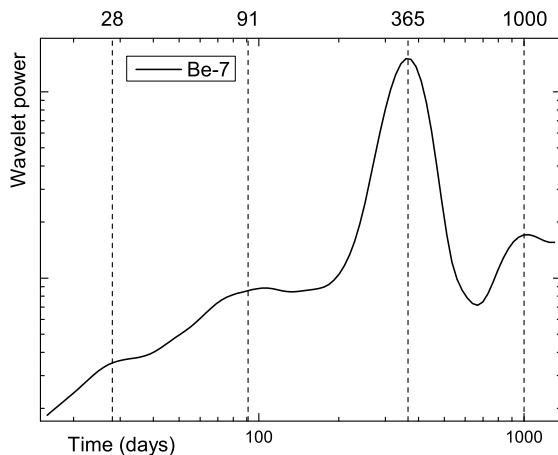


Figure 1: Wavelet spectrum of the  $^7\text{Be}$  specific activity in surface air, Helsinki.

Figure 2 shows a comparison of the  $^7\text{Be}$  and teleconnection indices WT spectra. In general, the teleconnection indices displayed a distinct annual period, and their visible peaks were positioned close to the seasonal and triennial  $^7\text{Be}$  periods

(Fig. 2). The spectral changes of the NAO and PNA indices were particularly consistent with the changes in the  $^7\text{Be}$  spectrum (with correlation coefficients of 0.7 and 0.6, respectively).

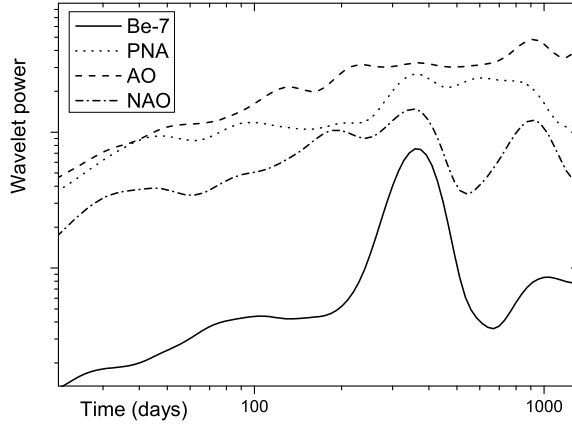


Figure 2: Wavelet transform spectra of the  $^7\text{Be}$  specific activity and teleconnection indices: Pacific/North American (PNA), Arctic Oscillation (AO), and North Atlantic Oscillation (NAO).

The meteorological data also showed a distinct annual peak, with additional peaks not coinciding with the  $^7\text{Be}$  periods (Fig. 3). The WT spectra for all temperature records, atmospheric pressure and sunspot number correlated well and significantly with the  $^7\text{Be}$  spectrum (with correlation coefficients larger than 0.9). The only time series not following the strong correlation pattern was precipitation. These findings could indicate that in general, the atmospheric conditions strongly influence the  $^7\text{Be}$  annual cycle, while temperature, atmospheric pressure, and sunspot number possibly have a bigger influence on the overall  $^7\text{Be}$  variations. The triennial  $^7\text{Be}$  cycle seems to be influenced by a combination of atmospheric conditions and teleconnections, which is in partial agreement with previous studies [6, 46, 62].

Finally, the data for tropopause height showed a good overall agreement

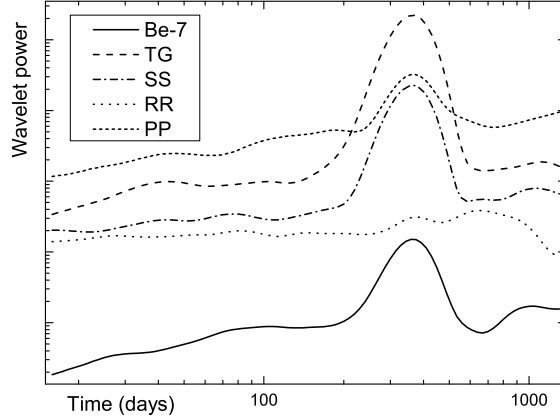


Figure 3: Wavelet transform spectra of the  $^7\text{Be}$  specific activity and meteorological data: mean daily temperature (TG), sunspot number (SS), precipitation (RR), and atmospheric pressure (PP).

with the  $^7\text{Be}$  cycles (with correlation coefficient larger than 0.9). As depicted in Fig. 4, the tropopause height records displayed a distinct annual peak, together with less evident monthly and seasonal peaks. The tropopause height gave a multiannual peak indicating a period somewhat shorter than the triennial  $^7\text{Be}$  peak. This tropopause height periodicity of  $\sim 2.5$  years has been identified previously [62]. A positive correlation between the tropopause height and the  $^7\text{Be}$  specific activity in surface air was observed by [17, 18, 50].

#### 4.2. Temporal dynamics of the $^7\text{Be}$ surface concentration

The  $^7\text{Be}$  periods found in WT analysis were further used in tddMA to investigate features of long-range dependence in the datasets. Specifically, the values of the Hurst exponents calculated on these intervals describe autocorrelation behavior of each investigated variable. In addition, a comparison of the local Hurst exponents of different variables on a given characteristic scale could unveil similarities in their dynamics.

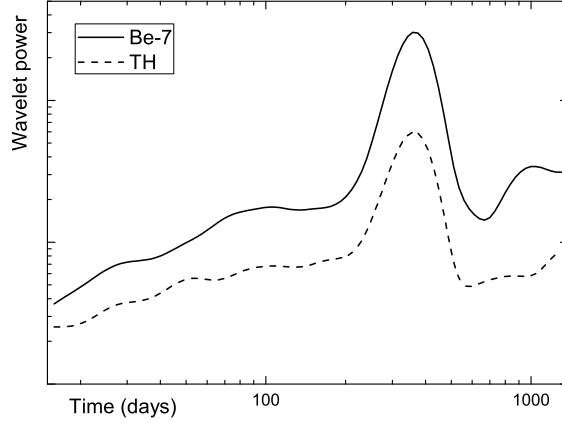


Figure 4: Wavelet transform spectra of the  ${}^7\text{Be}$  specific activity and tropopause height (TH).

Figure 5 shows the local Hurst exponents for the  ${}^7\text{Be}$  specific activity on its characteristic periods. On the shortest characteristic interval of one month, the exponents implied a strong autocorrelation, with the mean Hurst exponent of 0.72. With an increase in the characteristic period to three months, the mean Hurst exponent increased to 0.90, and this same pattern was repeated on the interval of one year – the mean Hurst exponent was 0.87, with no anticorrelation bouts. A significant change in the behavior of the local Hurst exponents occurred on the interval of three years, where we found a multiyear period with the exponents close to 0.5, followed by an anticorrelated regime. The mean Hurst exponent for this three-year period decreased to 0.58 (Fig. 5).

The local Hurst exponents on different characteristic intervals suggest that the temporal changes in the  ${}^7\text{Be}$  specific activity are most likely slow. Namely, the high values of the exponents on shorter time-scales of one and three months, and even one year, imply almost identical behavior in the  ${}^7\text{Be}$  records. For example, with the mean Hurst exponent of 0.90, within every trimester, the type of changes (i.e., an increase or decrease in the measured values) were almost the same as the type of changes within the preceding and subsequent trimester.

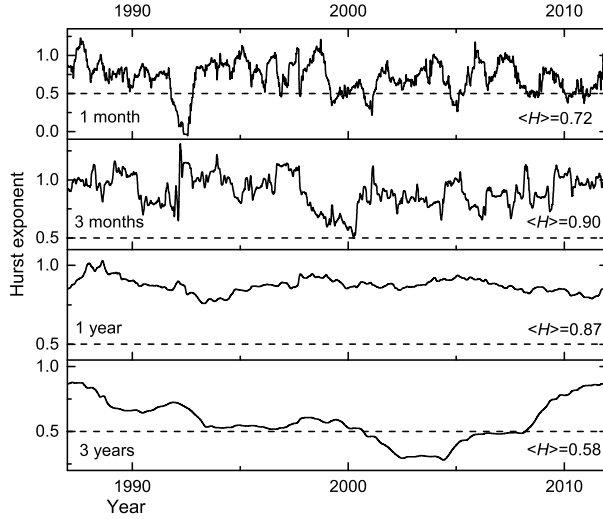


Figure 5: Local Hurst exponents and their mean values for the  ${}^7\text{Be}$  specific activity on its characteristic periods.

Similarly, the differences in the type of changes from one year to another also seemed negligible. Only over a prolonged period of time, which was three years in the case of the  ${}^7\text{Be}$  specific activity, we observed a variation in the  ${}^7\text{Be}$  dynamics: the highly correlated regime apparently shifted to slightly correlated, even anticorrelated behavior. This would suggest an existence of a crossover in the radionuclide's behavior on large (multiyear) scales that is maybe masked by the presence of a one-year peak in the  ${}^7\text{Be}$  wavelet spectrum.

#### 4.3. Comparative analysis of the variables' dynamics

To further analyze the observed behavior and possibly find a source of crossover in the  ${}^7\text{Be}$  dynamics, we compared its local Hurst exponents on the one- and three-year intervals with the exponents of the other investigated variables (Figs.6 and 7). Similarities in the temporal evolution of these Hurst exponents are described by the correlation functions also shown in Figs.6 and 7, with some characteristic values given in Table 1.

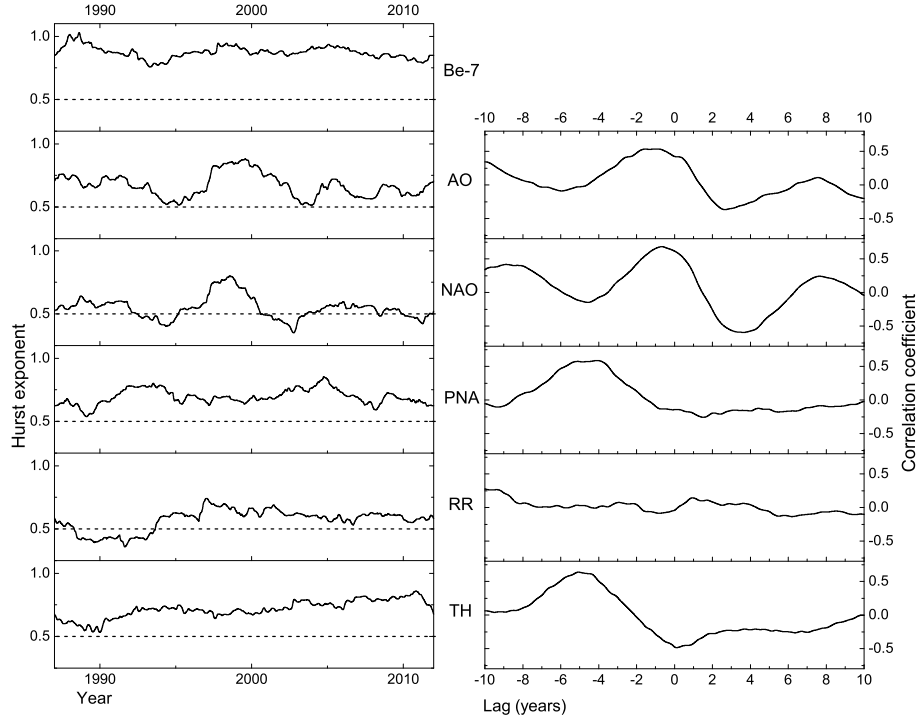


Figure 6: Left – local Hurst exponents on the one-year interval for (top to bottom): the  $^7\text{Be}$  specific activity, Arctic Oscillation, North Atlantic Oscillation, Pacific/North American, precipitation, and tropopause height, over 1987–2011. Right – correlation function between the local Hurst exponents of the  $^7\text{Be}$  specific activity and the corresponding variables.

#### 4.3.1. Dynamics over one year

On the one-year interval, the variables were autocorrelated, apart from NAO and precipitation over short periods (Fig.6). The minima of the correlation functions occurred when the  $^7\text{Be}$  specific activity was correlated with the corresponding variable’s values recorded later in time (Table 1). On the other hand, the maximum correlations showed a moderate to strong correlation (except precipitation) which occurred when the  $^7\text{Be}$  specific activity was correlated with the corresponding variable’s values recorded earlier in time. The strength of anticorrelation was less than the strength of correlation (i.e., the absolute value of the minimum was less than the absolute value of the maximum). These correla-

Table 1: The correlation value for time lag equal 0, maximum and minimum of the correlation functions given in Figs. 6 and 7. The time lags for which the minimum and maximum are reached are given in years. When time lag is positive, the  $^7\text{Be}$  specific activity is correlated with the corresponding variable's values recorded earlier in time (" $^7\text{Be}$  is in the future"), and vice versa.

Period	One year			Three years		
	corr. coeff. lag=0	maximum (lag in years)	minimum (lag in years)	corr. coeff. lag=0	maximum (lag in years)	minimum (lag in years)
AO	0.42	0.54 (-0.9)	-0.37 (2.7)	-0.02	0.19 (4.3)	-0.72 (-3.6)
NAO	0.61	0.68 (-0.7)	-0.60 (3.6)	-0.29	0.30 (10)	-0.71 (9.3)
PNA	-0.14	0.59 (-4.1)	-0.26 (1.5)	0.56	0.56 (0)	-0.51 (-4.8)
RR	-0.04	0.27 (-10)	-0.14 (6.2)	-0.52	0.45 (10)	-0.86 (3.4)
TH	-0.47	0.64 (-5.1)	-0.49 (0.1)	0.09	0.42 (-10)	-0.65 (6.1)

tion coefficients could imply that changes in the teleconnection indices reflected on the changes in the  $^7\text{Be}$  specific activity with a varying time lag: from less than a year for AO and NAO, to  $\sim 4$  years for PNA.

It is worth noting here that the extremes given in Table 1, which are found with the time lag of 10 years, should be taken with caution, as that time lag is at the very limit of the analyzed time window. This was the case with precipitation on the one-year interval, and NAO, precipitation and tropopause height on the three-year interval.

#### 4.3.2. Dynamics over three years

The long-range autocorrelations (on the three-year interval) give insight into the complexity of the variables' behavior (Fig. 7). While on the one-year interval, there were no significant variations in the type of changes in the  $^7\text{Be}$  specific activity from one year to the next, the temporal evolution was different on the three-year interval. Although the radionuclide's concentration showed strong autocorrelation prior to 1990 and after 2010, there were significant differences

during the period in-between. The transition in the correlation mode, from correlated to anticorrelated, occurred in all of the variables, except the tropopause height which was anticorrelated throughout the 1987–2011 period (Fig. 7).

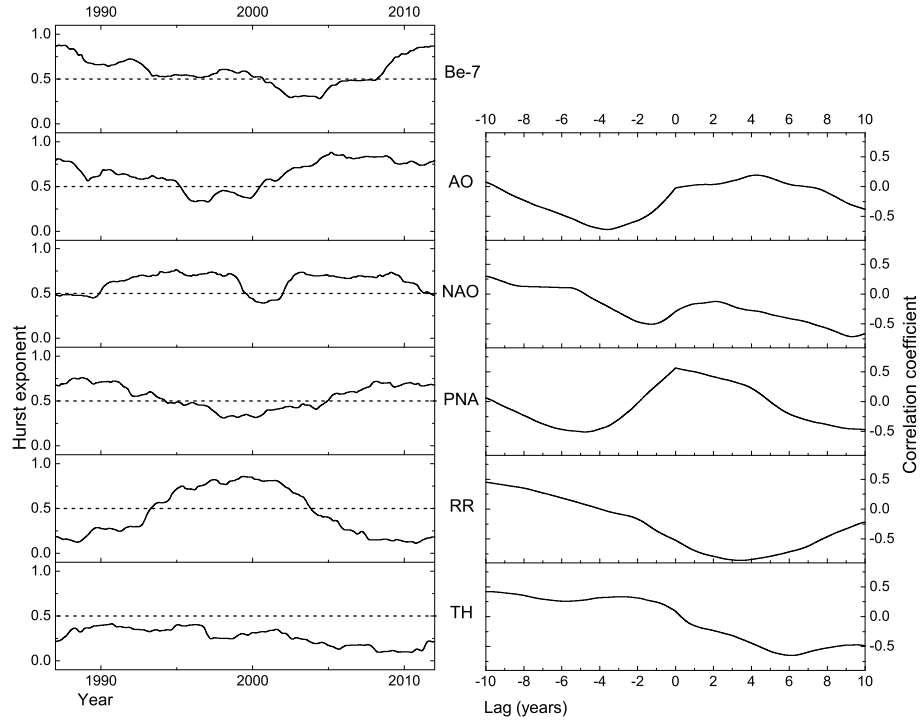


Figure 7: Same as Fig. 6 on the three-year interval.

During 1993–2005, the local  $^7\text{Be}$  Hurst exponent decreased, which may suggest that over this period there was a weakened effect of some global parameters, which have an impact on the dynamics of the  $^7\text{Be}$  specific activity. Over this period, AO, PNA and precipitation changed the mode, i.e. from correlated to anticorrelated, and vice versa. The transition of the AO and PNA teleconnection indices into the anticorrelated regime, which happened in  $\sim 1995$ , could have driven the  $^7\text{Be}$  specific activity shift into an anticorrelated regime. The correlation in the  $^7\text{Be}$  series was first reduced between 1995 and 2000, and the actual transition in the correlation mode (from correlated to anticorrelated) occurred

in 2000. Further evolution of the Hurst exponents showed that AO reversed back into the correlated regime in 2000, but the PNA reversal took another five years. The transition back into the correlated mode of the  $^7\text{Be}$  specific activity occurred later still, in 2008.

The maximum and minimum values of the correlation functions (Fig. 7 and Table 1) show that in contrast to the one-year interval, anticorrelation between the Hurst exponents of the investigated variables and the  $^7\text{Be}$  specific activity was stronger than their correlation. Further, the minima for the AO and PNA correlation functions occurred for a time lag of 4–5 years, which agrees with the aforementioned delay with which the mode reversals of the  $^7\text{Be}$  Hurst exponents followed the shifts in the teleconnections' autocorrelations (Fig. 7).

The slow changes in the dynamics of the  $^7\text{Be}$  specific activity could be interconnected with the changes in the teleconnections. In one scenario of the interconnection, a direct influence of the indices on the  $^7\text{Be}$  specific activity could be assumed. This scenario would then suggest a relatively long response time (4–5 years) in which the correlation changes in large-scale atmospheric circulation were mirrored by the correlation changes in the radionuclide activity. On the other hand, if the teleconnection indices and  $^7\text{Be}$  specific activity had a common driving mechanism, then the changes would first occur in the behavior of AO, then PNA and  $^7\text{Be}$  specific activity (Fig. 7). The correlation mode shifts for AO and PNA were not only earlier, but also faster (note a prolonged period in the second half of the 1990s during which the  $^7\text{Be}$  Hurst exponent hovered close to 0.5). This slow reaction of the  $^7\text{Be}$  specific activity to a driving mechanism would result from additional forces that dampen the influence and thus prolong the response time. Another potential interconnection between the variables is a combination of the two scenarios, encompassing a common driving mechanism and an influence that teleconnections exert on the  $^7\text{Be}$  specific activity in surface air.

A possible explanation for the observed change in the correlation of the variables (Fig. 7) could lie in the solar activity during 1993–2005. This period encompassed the end of solar cycle 22 (1986–1996) and most of solar cycle 23

(1996–2008). In contrast to solar cycle 22 with high solar activity, solar cycle 23 was noticeably smaller [63], and the changes in correlation modes could reflect those changes in solar activity. It is worth noting here that over 1993–2005, the decrease in the correlation of the  $^7\text{Be}$  series was not associated with a decrease in the measured  $^7\text{Be}$  specific activity. A major influence of solar forcing on the  $^7\text{Be}$  surface concentration for timescales longer than one year has been noticed by [64].

It is also interesting to note that the precipitation Hurst exponents on the three-year period (Fig. 7) showed a decrease in anticorrelation from 1987 to 1994, and an increase in anticorrelation from 2006 to 2011, just as the Hurst exponents of the  $^7\text{Be}$  specific activity exhibited the opposite behavior. Over the period in-between, 1994–2006, precipitation was autocorrelated while the  $^7\text{Be}$  Hurst exponent hovered around 0.5 and then shifted into anticorrelation (Fig. 7). Further, very strong anticorrelation between the precipitation and  $^7\text{Be}$  Hurst exponents of -0.86 was noted with a time lag of approximately three years (Table 1).

Finally, some caveats in our analysis should be mentioned. The availability of the  $^7\text{Be}$  data limited the analysis to time periods from ten days to four years, not allowing investigation of periodicities on shorter time scales, such as the cycles found in a wavelet analysis of daily  $^7\text{Be}$  concentrations [54]. It also limited our insight into longer, multiannual or interdecadal, periodicities reported in [45]. Moreover, WT spectral analysis is a linear method which detects linear combinations of characteristic frequencies unless their magnitude is very small [53]. Further studies should aim at improvements that look into recognition of these linear combinations, and their separation from true characteristic frequencies inherent to the data. The future modelling efforts could possibly profit from the results of the comparison of the WT spectra of the  $^7\text{Be}$  specific activity, meteorological parameters, and teleconnection indices, and use our findings for re-calibration of modelling strategies.

Further, in our analysis an emphasis was given to an interrelationship between the  $^7\text{Be}$  specific activity and other parameters. A mutual linkage between

the parameters was not discussed, although our results offered some ready conclusions. For example, on the short characteristic intervals of one and three months, all teleconnection indices were autocorrelated (not shown), while periods of anticorrelation first occurred in NAO on the one-year interval (Fig. 6) and then in AO and PNA on the three-year interval (Fig. 7). These results imply a very similar behavior between the AO and PNA teleconnections and the  $^7\text{Be}$  specific activity, including slow changes which become evident only on the three-year interval.

## 5. Conclusions

Wavelet transform spectral analysis revealed the existence of four characteristic periods in the  $^7\text{Be}$  specific activity: a one-month cycle, a three-month cycle, an annual cycle, and a triennial cycle. Our results implied that the tropopause height, atmospheric conditions (especially temperature), atmospheric pressure, and the sunspot number, significantly influence the overall  $^7\text{Be}$  spectral behavior. The seasonal period also seems to be influenced by large-scale atmospheric circulation, particularly by the NAO and PNA indices, and by the tropopause height, which seems to also influence the monthly  $^7\text{Be}$  period. The triennial  $^7\text{Be}$  cycle is likely to be influenced by a combination of atmospheric conditions and teleconnections. In our data, the characteristic time periods of the NAO and PNA patterns seemed to match the periods of the radionuclide's activity better than AO.

Local Hurst exponent analysis offered further insight into the complex dynamic of the  $^7\text{Be}$  specific activity in surface air and its relationship to dynamics of meteorological parameters and teleconnection indices. Comparisons were made on the  $^7\text{Be}$  specific activity characteristic periods of one year and three years. On the time period of one year and shorter, the  $^7\text{Be}$  specific activity was strongly autocorrelated. The longest, three-year interval, showed some periods of anticorrelation implying that changes in the dynamics of this radionuclide are slow and evident only on the scale of three years. Similarities in the overall

pattern of the Hurst exponents on the four characteristic intervals suggest a good agreement in the AO, PNA and  $^7\text{Be}$  specific activity behavior.

### Acknowledgements

This paper was realized within the following projects: "Advanced analytical, numerical and methods of analysis of fluid mechanics and complex systems" (No. OI174014), "Phase transitions and characterization of inorganic and organic systems" (No. OI171015), and "Climate changes and their influence on the environment: impacts, adaptation and mitigation" (No. III43007), financed by the Ministry of Education, Science and Technological Development of the Republic of Serbia (2011-2016). Suzana Blesić has received funding from the European Unions Horizon 2020 research and innovation programme under the Marie Skłodowska-Curie grant agreement No. 701785. The authors would like to thank the REM group for provision of the beryllium-7 specific activity measurements from the REM data base (REmdb at the Institute of Transuranium Elements, REM group, DJ JRC Ispra site, European Commission).

### References

### References

- [1] D. Lal, B. Peters, Cosmic ray produced radioactivity on the Earth, in: K. Sitte (Ed.), Kosmische Strahlung II / Cosmic Rays II, Vol. 9 / 46 / 2 of Handbuch der Physik / Encyclopedia of Physics, Springer Berlin Heidelberg, 1967, pp. 551–612. doi:10.1007/978-3-642-46079-1\_7.
- [2] D. M. Koch, D. J. Jacob, W. C. Graustein, Vertical transport of tropospheric aerosols as indicated by  $^7\text{Be}$  and  $^{210}\text{Pb}$  in a chemical tracer model, J. Geophys. Res. 101 (D13) (1996) 18651–18666. doi:10.1029/96JD01176.
- [3] T. Tokieda, K. Yamanaka, K. Harada, S. Tsunogai, Seasonal variations of residence time and upper atmospheric contribution of aerosols

- studied with Pb-210, Bi-210, Po-210 and Be-7, *Tellus B* 48 (5).  
doi:10.1034/j.1600-0889.1996.t01-4-00006.x.
- [4] C. Dueñas, M. Fernández, J. Carretero, E. Liger, S. Cañete, Long-term variation of the concentrations of long-lived Rn descendants and cosmogenic  $^7\text{Be}$  and determination of the MRT of aerosols, *Atmos. Environ.* 38 (9) (2004) 1291–1301.
- [5] U. Heikkilä, J. Beer, V. Alfimov, Beryllium-10 and beryllium-7 in precipitation in Dübendorf (440 m) and at Jungfrauoch (3580 m), Switzerland (1998-2005), *J. Geophys. Res.* 113 (D11). doi:10.1029/2007JD009160.
- [6] E. Gerasopoulos, C. Zerefos, C. Papastefanou, P. Zanis, K. O'Brien, Low-frequency variability of beryllium-7 surface concentrations over the Eastern Mediterranean, *Atmos. Environ.* 37 (13) (2003) 1745–1756.
- [7] P. Cristofanelli, P. Bonasoni, L. Tositti, U. Bonafè, F. Calzolari, F. Evangelisti, S. Sandrini, A. Stohl, A 6-year analysis of stratospheric intrusions and their influence on ozone at Mt. Cimone (2165 m above sea level), *J. Geophys. Res.* 111 (D3) (2006), d03306. doi:10.1029/2005JD006553.
- [8] H. W. Feely, R. J. Larsen, C. G. Sanderson, Factors that cause seasonal variations in Beryllium-7 concentrations in surface air, *J. Environ. Radioact.* 9 (3) (1989) 223–249.
- [9] F. Cannizzaro, G. Greco, M. Raneli, M. Spitale, E. Tomarchio, Concentration measurements of  $^7\text{Be}$  at ground level air at Palermo, Italy—comparison with solar activity over a period of 21 years, *J. Environ. Radioact.* 72 (3) (2004) 259–271.
- [10] M. K. Pham, M. Betti, H. Nies, P. P. Povinec, Temporal changes of  $^7\text{Be}$ ,  $^{137}\text{Cs}$  and  $^{210}\text{Pb}$  activity concentrations in surface air at Monaco and their correlation with meteorological parameters, *J. Environ. Radioact.* 102 (11) (2011) 1045–1054.

- [11] L. Bourcier, O. Masson, P. Laj, J. Pichon, P. Paulat, E. Freney, K. Sellegri, Comparative trends and seasonal variation of  $^7\text{Be}$ ,  $^{210}\text{Pb}$  and  $^{137}\text{Cs}$  at two altitude sites in the central part of France, *J. Environ. Radioact.* 102 (3) (2011) 294–301.
- [12] P. Zanis, E. Gerasopoulos, A. Priller, C. Schnabel, A. Stohl, C. Zerefos, H. Gäggeler, L. Tobler, P. Kubik, H. Kanter, H. Scheel, J. Luterbacher, M. Berger, An estimate of the impact of stratosphere-to-troposphere transport (STT) on the lower free tropospheric ozone over the Alps using  $^{10}\text{Be}$  and  $^7\text{Be}$  measurements, *J. Geophys. Res.* 108 (D12) (2003), 8520. doi:10.1029/2002JD002604.
- [13] D. Todorovic, D. Popovic, G. Djuric, Concentration measurements of  $^7\text{Be}$  and  $^{137}\text{Cs}$  in ground level air in the Belgrade City area, *Environ. Internat.* 25 (1) (1999) 59–66.
- [14] S. Daish, A. Dale, C. Dale, R. May, J. Rowe, The temporal variations of  $^7\text{Be}$ ,  $^{210}\text{Pb}$  and  $^{210}\text{Po}$  in air in England, *J. Environ. Radioact.* 84 (3) (2005) 457–467.
- [15] M. Yoshimori, Production and behavior of beryllium 7 radionuclide in the upper atmosphere, *Adv. Space Res.* 36 (5) (2005) 922–926.
- [16] C. Papastefanou, Beryllium-7 aerosols in ambient air, *Aerosol Air Qual. Res.* 9 (2) (2009) 187–197.
- [17] E. Gerasopoulos, P. Zanis, A. Stohl, C. Zerefos, C. Papastefanou, W. Ringer, L. Tobler, S. Hübener, H. Gäggeler, H. Kanter, L. Tositti, S. Sandrini, A climatology of  $^7\text{Be}$  at four high-altitude stations at the Alps and the Northern Apennines, *Atmos. Environ.* 35 (36) (2001) 6347–6360.
- [18] A. Ioannidou, A. Vasileiadis, D. Melas, Time lag between the tropopause height and  $^7\text{Be}$  activity concentrations on surface air, *J. Environ. Radioact.* 129 (2014) 80–85.

- [19] A. Kulan, A. Aldahan, G. Possnert, I. Vintersved, Distribution of  $^7\text{Be}$  in surface air of Europe, *Atmos. Environ.* 40 (21) (2006) 3855–3868.
- [20] B. R. Persson, E. Holm,  $^7\text{Be}$ ,  $^{210}\text{Pb}$ , and  $^{210}\text{Po}$  in the surface air from the Arctic to Antarctica, *J. Environ. Radioact.* 138 (2014) 364–374.
- [21] M. Hernández-Ceballos, G. Cinelli, M. M. Ferrer, T. Tollefsen, L. D. Felice, E. Nweke, P. Tognoli, S. Vanzo, M. D. Cort, A climatology of  $^7\text{Be}$  in surface air in European Union, *J. Environ. Radioact.* 141 (2015) 62–70.
- [22] C. Papastefanou, A. Ioannidou, Depositional fluxes and other physical characteristics of atmospheric beryllium-7 in the temperate zones ( $40^\circ\text{N}$ ) with a dry (precipitation-free) climate, *Atmos. Environ.* 25 (10) (1991) 2335–2343.
- [23] A. Ioannidou, C. Papastefanou, Precipitation scavenging of  $^7\text{Be}$  and  $^{137}\text{Cs}$  radionuclides in air, *J. Environ. Radioact.* 85 (1) (2006) 121–136.
- [24] F. Cannizzaro, G. Greco, M. Raneli, M. C. Spitale, E. Tomarchio, Behaviour of  $^7\text{Be}$  air concentration observed during a period of 13 years and comparison with sun activity, *Nucl. Geophys.* 9 (1995) 597–607. doi:10.1016/0969-8086(95)00043-7.
- [25] N. Ali, E. Khan, P. Akhter, N. Khattak, F. Khan, M. Rana, The effect of air mass origin on the ambient concentrations of  $^7\text{Be}$  and  $^{210}\text{Pb}$  in Islamabad, Pakistan, *J. Environ. Radioact.* 102 (1) (2011) 35–42.
- [26] J. Chao, Y. Chiu, H. Lee, M. Lee, Deposition of beryllium-7 in Hsinchu, Taiwan, *Appl. Radiat. Isot.* 70 (2) (2012) 415–422.
- [27] F. Piñero García, M. Ferro García, M. Azahra,  $^7\text{Be}$  behaviour in the atmosphere of the city of Granada January 2005 to December 2009, *Atmos. Environ.* 47 (2012) 84–91.
- [28] D. Todorovic, D. Popovic, J. Nikolic, J. Ajtic, Radioactivity monitoring in ground level air in Belgrade urban area, *Radiat. Prot. Dosim.* 142 (2-4) (2010) 308–313. doi:10.1093/rpd/ncq211.

- [29] J. Ajtić, D. Todorović, A. Filipović, J. Nikolić, Ground level air beryllium-7 and ozone in Belgrade, *Nucl. Technol. Radiat.* 23 (2) (2008) 65–71. doi:10.2298/NTRP0802065A.
- [30] J. V. Ajtić, D. J. Todorović, J. D. Nikolić, V. S. Đurđević, Ground level air beryllium-7 and ozone in Belgrade, *Nucl. Technol. Radiat.* 28 (4) (2013) 381–388. doi:10.2298/NTRP1304381A.
- [31] S. M. Papandreou, M. I. Savva, K. L. Karfopoulos, D. J. Karangelos, M. J. Anagnostakis, S. E. Simopoulos, Monitoring of  $^7\text{Be}$  atmospheric activity concentration using short term measurements, *Nucl. Technol. Radiat.* 26 (2) (2011) 101–109. doi:10.2298/NTRP1102101P.
- [32] A. C. Carvalho, M. Reis, L. Silva, M. J. Madruga, A decade of  $^7\text{Be}$  and  $^{210}\text{Pb}$  activity in surface aerosols measured over the Western Iberian Peninsula, *Atmos. Environ.* 67 (0) (2013) 193–202.
- [33] R. Lozano, M. Hernández-Ceballos, J. Rodrigo, E. S. Miguel, M. Casas-Ruiz, R. García-Tenorio, J. Bolívar, Mesoscale behavior of  $^7\text{Be}$  and  $^{210}\text{Pb}$  in superficial air along the Gulf of Cadiz (south of Iberian Peninsula), *Atmos. Environ.* 80 (2013) 75–84.
- [34] L. Tositti, E. Brattich, G. Cinelli, D. Baldacci, 12 years of  $^7\text{Be}$  and  $^{210}\text{Pb}$  in Mt. Cimone, and their correlation with meteorological parameters, *Atmos. Environ.* 87 (2014) 108–122.
- [35] J. M. Wallace, D. S. Gutzler, Teleconnections in the Geopotential Height Field during the Northern Hemisphere Winter, *Mon. Wea. Rev.* 109 (4) (1981) 784–812.
- [36] A. G. Barnston, R. E. Livezey, Classification, seasonality and persistence of low-frequency atmospheric circulation patterns, *Mon. Wea. Rev.* 115 (6) (1987) 1083–1126.

- [37] J. W. Hurrell, Decadal trends in the north atlantic oscillation: Regional temperatures and precipitation, *Science* 269 (5224) (1995) 676–679. doi:10.1126/science.269.5224.676.
- [38] M. H. P. Ambaum, B. J. Hoskins, D. B. Stephenson, Arctic Oscillation or North Atlantic Oscillation?, *J. Clim.* 14 (16) (2001) 3495–3507.
- [39] J. M. Wallace, North atlantic oscillation annular mode: Two paradigms—one phenomenon, *Q. J. R. Meteorol. Soc.* 126 (564) (2000) 791–805. doi:10.1002/qj.49712656402.
- [40] D. J. Leathers, B. Yarnal, M. A. Palecki, The Pacific/North American teleconnection pattern and United States climate. Part I: Regional temperature and precipitation associations, *J. Clim.* 4 (5) (1991) 517–528.
- [41] D. J. Leathers, M. A. Palecki, The Pacific/North American teleconnection pattern and United States climate. Part II: Temporal characteristics and index specification, *J. Clim.* 5 (7) (1992) 707–716.
- [42] D. W. J. Thompson, J. M. Wallace, The Arctic Oscillation signature in the wintertime geopotential height and temperature fields, *Geophys. Res. Lett.* 25 (9) (1998) 1297–1300. doi:10.1029/98GL00950.
- [43] R. W. Higgins, A. Leetmaa, V. E. Kousky, Relationships between climate variability and winter temperature extremes in the United States, *J. Clim.* 15 (13) (2002) 1555–1572.
- [44] J. Hedfors, A. Aldahan, A. Kulan, G. Possnert, K.-G. Karlsson, I. Vintarsved, Clouds and  $^7\text{Be}$ : Perusing connections between cosmic rays and climate, *J. Geophys. Res.* 111 (D2), d02208. doi:10.1029/2005JD005903.
- [45] A.-P. Leppänen, A. Pacini, I. Usoskin, A. Aldahan, E. Echer, H. Evangelista, S. Klemola, G. Kovaltsov, K. Mursula, G. Possnert, Cosmogenic  $^7\text{Be}$  in air: A complex mixture of production and transport, *J. Atmos. Sol-Terr. Phy.* 72 (13) (2010) 1036–1043.

- [46] A.-P. Leppänen, I. Usoskin, G. Kovaltsov, J. Paatero, Cosmogenic  $^7\text{Be}$  and  $^{22}\text{Na}$  in Finland: Production, observed periodicities and the connection to climatic phenomena, *J. Atmos. Sol-Terr. Phy.* 74 (2012) 164–180.
- [47] A.-P. Leppänen, J. Paatero,  $^7\text{Be}$  in Finland during the 1999-2001 Solar maximum and 2007-2009 Solar minimum, *J. Atmos. Sol-Terr. Phy.* 97 (2013) 1–10.
- [48] J.-F. Lamarque, P. G. Hess, Arctic oscillation modulation of the northern hemisphere spring tropospheric ozone, *Geophys. Res. Lett.* 31 (6) (2004), 106127. doi:10.1029/2003GL019116.
- [49] M. Hernández-Ceballos, G. Cinelli, T. Tollefsen, M. Marín-Ferrer, Identification of airborne radioactive spatial patterns in Europe – Feasibility study using Beryllium-7, *J. Environ. Radioact.* 155–156 (2016) 55–62.
- [50] M. Hernández-Ceballos, E. Brattich, G. Cinelli, J. Ajtić, V. Djurdjević, Seasonality of  $^7\text{Be}$  concentrations in Europe and influence of tropopause height, *Tellus B* 2016, 68, 29534. doi:10.3402/tellusb.v68.29534.
- [51] A. K. Tank, J. Wijngaard, G. Können, R. Böhm, G. Demarée, A. Gocheva, M. Mileta, S. Pashiardis, L. Hejkrlik, C. Kern-Hansen, R. Heino, P. Bessemoulin, G. Müller-Westermeier, M. Tzanakou, S. Szalai, T. Pálsdóttir, D. Fitzgerald, S. Rubin, M. Capaldo, M. Maugeri, A. Leitass, A. Bukantis, R. Aberfeld, A. van Engelen, E. Forland, M. Mietus, F. Coelho, C. Mares, V. Razuvaev, E. Nieplova, T. Cegnar, J. Antonio López, B. Dahlström, A. Moberg, W. Kirchhofer, A. Ceylan, O. Pachaliuk, L. Alexander, P. Petrovic, Daily dataset of 20th-century surface air temperature and precipitation series for the European Climate Assessment, *Int. J. Climatol.* 22 (12) (2002) 1441–1453. doi:10.1002/joc.773.
- [52] E. Kalnay, M. Kanamitsu, R. Kistler, W. Collins, D. Deaven, L. Gandin, M. Iredell, S. Saha, G. White, J. Woollen, Y. Zhu, M. Chelliah, W. Ebisuzaki, W. Higgins, J. Janowiak, K. C. Mo, C. Ropelewski, J. Wang,

- A. Leetmaa, R. Reynolds, Roy Jenne, D. Joseph, The NCEP/NCAR 40-year reanalysis project, *Bull. Am. Meteorol. Soc.* 77 (3) (1996) 437–471.
- [53] M. Bračić, A. Stefanovska, Wavelet-based analysis of human blood-flow dynamics, *Bull. Math. Biol.* 60 (5) (1998) 919–935. doi:10.1006/bulm.1998.0047.
- [54] S. Kikuchi, H. Sakurai, S. Gunji, F. Tokanai, Temporal variation of  $^7\text{Be}$  concentrations in atmosphere for 8 y from 2000 at Yamagata, Japan: solar influence on the  $^7\text{Be}$  time series, *J. Environ. Radioact.* 100 (2009) 515–521. doi:10.1016/j.jenvrad.2009.03.017.
- [55] C. Torrence, G. P. Compo, A practical guide to wavelet analysis, *Bull. Am. Meteorol. Soc.* 79 (1) (1998) 61–78.
- [56] J. Lewalle, M. Farge, K. Schneider, Wavelet transforms, in: C. Tropea, A. Yarin, J. Foss (Eds.), *Handbook of Experimental Fluid Mechanics*, Springer-Verlag, Berlin Heidelberg, 2007, pp. 1378–1398.
- [57] D. Stratimirović, S. Milošević, S. Blesić, M. Ljubisavljević, Wavelet analysis of discharge dynamics of fusimotor neurons, *Phys. A* 291 (1-4) (2001) 13–23.
- [58] A. Carbone, G. Castelli, H. Stanley, Time-dependent Hurst exponent in financial time series, *Phys. A* 344 (1-2) (2004) 267–271.
- [59] G. Consolini, R. De Marco, P. De Michelis, Intermittency and multifractal Brownian character of geomagnetic time series, *Nonlinear Proc. Geoph.* 20 (4) (2013) 455–466. doi:10.5194/npg-20-455-2013.
- [60] C.-K. Peng, J. Mietus, J. Hausdorff, S. Havlin, H. Stanley, A. Goldberger, Long-range anticorrelations and non-gaussian behavior of the heartbeat, *Phys. Rev. Lett.* 70 (9) (1993) 1343–1346. doi:10.1103/PhysRevLett.70.1343.

- [61] M. Yamamoto, A. Sakaguchi, K. Sasaki, K. Hirose, Y. Igarashi, C. K. Kim, Seasonal and spatial variation of atmospheric  $^{210}\text{Pb}$  and  $^7\text{Be}$  deposition: features of the Japan Sea side of Japan, *J. Environ. Radioact.* 86 (1) (2006) 110–131.
- [62] J. Angell, J. Korshover, Quasi-biennial variations in temperature, total ozone, and tropopause height, *J. Atmos. Sci.* 21 (5) (1964) 479–492.
- [63] NASA (National Aeronautics and Space Administration), Marshall Space Flight Center, <http://solarscience.msfc.nasa.gov/predict.shtml> visited on 28 June 2015.
- [64] S. Talpos, N. Rimbu, D. Borsan, Solar forcing on the  $^7\text{Be}$ -air concentration variability at ground level, *J. Atmos. Sol.-Terr. Phys.* 67 (16) (2005) 1626–1631.